REAL TIME PERFORMANCE INVESTIGATION OF EXTENDED PHASE SHIFTED DUAL ACTIVE BRIDGE CONVERTER IN DC-MICROGRID WITH OPTIMUM OPERATING ZONE

anupam.KUMAR
Research Scholar, Department of Electrical Engineering
National Institute of Technology, Srinagar
Jammu &Kashmir,India
kanupam310@gmail.com

abdul.HAMID BHAT
Professor, Department of Electrical Engineering
National Institute of Technology, Srinagar
Jammu & Kashmir, India
bhatdee@nitsri.net

pramod.AGARWAL
Professor,Department of Electrical Engineering
Indian Institute of Technology, Roorkee
Uttarakhand, India
pramgfee@iitr.ac.in

Abstract: *In this paper real time performance investigation of Dual active bridge (DAB) (300:100,2 KVA) converter with Extended Phase Shift (EPS) is done with storage element (battery) at the low voltage (LV) DC-bus and solar photovoltaic cell on the high voltage (HV) DC- bus .Linear Load connected at the HV bus is supplied from the source and when the load demand increases storage element (battery) discharges through the DAB and energy flows from the LV bus to the HV bus via the DAB. Dual Active Bridge is operated in Extended Phase Shift (EPS) mode. A closed loop controller having load voltage as target variable is used for providing the required outer phase shift between the H-bridges. Main contributions of this work are real time performance investigation of DAB for bidirectional flow of power, closed loop operation of DAB and its real time evaluation and obtaining the optimum duty ratio through the controller. State of charge, battery voltage and battery current are obtained. DAB waveforms (Primary voltage, Secondary Voltage, Inductor current and voltage) are also obtained. Simulation studies for the above mentioned system is carried out in MATLAB and are aptly verified with real time simulation results obtained through OPAL-RT.*

Keywords: *Dual active bridge converter, extended phase shift, closed loop controller, operating zone, DC-Microgrid, OPAL-RT, State of charge, Real time evaluation*

1. Introduction

Microgrids are defined as a local integrated network comprising of Energy sources, storage elements and interconnected loads. Based upon the bus type (AC,DC,both) onto which power electronics interface is connected the microgrids are classified as DC,AC or hybrid microgrid[1]. Power electronics interface plays a crucial role in providing stability to dc microgrids by maintaining steady and bidirectional flow of power and maintaining the load voltage at the desired value. Various bidirectional converters along with their control strategies [2] have been discussed. A boost converter was used in dc microgrid for boosting the voltage of renewable source to match the voltage level of DC bus [3].In [3] the boost converter is used to interface PV (Photovoltaic) source to dc voltage bus. The boost converter used in [3] is unidirectional and only the converter waveforms are shown. In [4] the control of batteries connected in parallel to a dc-microgrid is shown. Load division among batteries is done along-with securing a safe terminal voltage for batteries and avoiding overload. In [4] a bidirectional buck-boost converter is implemented for controlling the charge and discharge of batteries and current stabilisation. Battery equalisation and current sharing for both the batteries are also plotted in [4]. In [5] a droop controller for dc-dc converter is developed, modal and sensitivity analysis of multi-terminal dc grids is performed for considering the interactions between the different controllers.

Dual active bridge [DAB] converter is a bidirectional converter introduced for the purpose of bidirectional power flow with improved efficiency, reduced size and low cost [6]. DAB operates in four phase shifted modulation schemes namely single phase shift (SPS), Extended phase shift (EPS), Dual phase shift (DPS) and triple phase shift (TPS). A comprehensive comparative analysis of DAB operating in SPS and EPS mode based upon its application as Solid state transformer is shown in [7].Also in [7] the comparative analysis of DAB

based upon peak current stress and transmission power is carried out. Application of DAB in battery storage connected PV(Photovoltaic) source is shown in [8], converter waveforms(primary voltage, secondary voltage etc) for DAB operating in EPS mode are obtained, but only simulations results are presented and none of the battery characteristics are obtained or discussed. SPS modulation strategy is the basic technique in which power flow is carried out depending on the phase-shift between the two H-bridges as discussed in [9-10]. In [10] the steady state average model along with small signal average model are developed for DAB operating in SPS mode and discussed along with a detailed analysis of design and control of DAB. After this EPS modulation strategy was discussed in [11] regarding its application in aerospace energy storage system. In [11] the performance of DAB is evaluated based on its ZVS (Zero Voltage Switching) operating range and experimental results are obtained for SPS and EPS mode for light linear load applied at DAB converter's secondary side. A detailed study of backflow power and converter operation along-with its basic characterization supported by experimental results for DAB working in EPS mode is shown in [12].

In [13] a hybrid controller for DAB is proposed for the converter combining a phase shift modulation and variable duty ratio over the whole ZVS range.

In [14] a controller having the combined benefits of a conventional phase shift controller and a burst controller is used for extending the ZVS range of all switches whenever a variation in either primary or secondary voltage appears.

Double phase shift modulation strategy for control of DAB is introduced in [15] and DPS based mathematical model of DAB is proposed in [16].

TPS based DAB is proposed in [17] and a generalised small signal linear model of TPS based DAB incorporating phase shift in duty ratio is developed. A multi input state space model of TPS based DAB is proposed in [18].In [19] an accurate average model of DAB is developed for application in acausal systems, the developed model incorporates the switching dynamics thus making the model suitable for control and power applications.

In [20] a small signal model of a PFC(power factor correction) plus dual active bridge converter topology is studied in detail and a full order state space model is developed describing the VSF(Variable switching frequency) control. In the proposed topology the bulky DC link voltage is eliminated. Simulation and experimental models of the proposed topology are also presented.

Vehicle to grid technology is developed in [21] and application of DAB as a bidirectional DC charger for electric vehicle is shown. A charging control methodology is proposed and simulation results are presented for the above mentioned controller.

Based on the above literature survey the following contributions are made in the present work:

(a)A study, design and control of DC microgrid is proposed.

(b)Bidirectional flow of power through DAB is shown along-with DAB characteristics.

(c) Battery characteristics of battery storage system connected at the low voltage side of DAB is obtained.

(d)Controller operation and performance for regulating load voltage and subsequently providing the optimum duty ratio for converter operation is done.

(e)Optimum operating duty ratio for converter operating in EPS mode is obtained.

(f) Real time experimental results for above mentioned controller and DAB operating in Extended Phase shift mode is obtained.

2. DC Microgrid

A microgrid in which the power electronics interface is connected to the dc bus is classified as DC microgrid. The schematic diagram of DC-microgrid studied in the present work is shown in Fig.1. It consists of a renewable energy source (ex. Solar PV array) connected at the high voltage bus. The power electronics interface (DAB) is connected between the HV (high voltage) bus and LV (low voltage) bus. The load is connected at the high voltage bus. The solar PV array has a maximum power rating of 1000VA. The battery storage system consists of two batteries connected in series each having a voltage rating of 34V. The closed loop controller regulates the output load voltage to the desired level. The PV array feeds the load and stores energy in battery storage system under normal operating condition. When the load demand is increased keeping the input power same, battery discharges and thus the increased load demand is met. The closed loop controller regulates the load voltage as well as the the battery voltage.

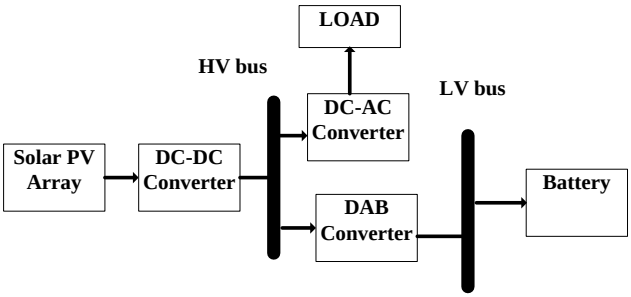

Fig.1.Application of dual active bridge converter in DC Micro-grid

2(a). System Design and modelling

In this section the whole dc-microgrid is explicated in details. The design and modelling of Solar PV system, DAB converter and battery storage system

(a)PV System design:

The PV system has been modelled previously and the designed model along-with governing equations for design of different components are presented in[22]. Photo Voltaic (PV) energy system contains PV modules or arrays, which convert solar energy in the form of solar irradiation into electrical energy. Photovoltaic cell is the smallest block of a PV system and they are connected in series and parallel thus forming a PV module. A PV module generally consists of 36 or 76 cells. After this PV modules are combined in series and parallel to form PV arrays. From [22] the following design equations are used for the design of Solar PV.

Equivalent circuit of PV cell has a current source (photocurrent), a diode parallel to it, a resistor in series describing an internal resistance to the flow of current and a shunt resistance connected across it.

The current (I) supplied to the load can be given as in equation (1).

$$\left[e^{\text{—}} \quad 1\right] \qquad (1)$$

Where

= current generated by the incident light, I_d = diode current = $\left[e^{\text{—}} \quad 1\right]$

$I_{0,\,cell}$ = reverse saturation or leakage current of the diode, q = electron charge = (1.60217646 × 10−19 C), k=Boltzmann constant = (1.3806503 × 10−23 J/K), T =temperature of the *p–n* junction in Kelvin, a = diode ideality constant, I_{sh}= current through shunt resistance

The PV link capacitor in terms of PV voltage is expressed as (2).

(2)

(b) Boost converter design

The duty ratio (D) of operation for boost converter having solar PV output voltage (V_{pv}) as input and HV side DC bus voltage($V_{\ v}$) as output is expressed as:

$$_t=1 \quad \text{—} \qquad (3)$$

The inductance value for the the boost converter to operate in continuous conduction mode (CCM) is:

$$\text{————} \qquad (4)$$

$_t$=Duty ratio of operation, V_{pv}=PV output voltage, $_{pv}$=Minimum ripple allowed in input current.

(c)Design of DAB and its modelling in EPS mode.

From the power circuit diagram of a Single phase dual active bridge converter shown in Fig.2, it can be seen that DAB consists of two back-to-back connected DC/AC converters connected through a high frequency transformer.

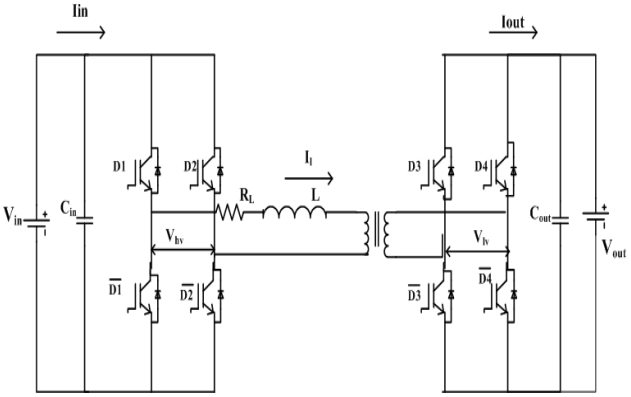

Fig.2. Power circuit diagram of single-phase dual active bridge converter depicting input and output voltages.

The inductor is a combination of primary side inductance plus the secondary side inductance referred to primary side. Each bridge is operated with a duty ratio of 50%.

Now modelling of DAB operating in EPS mode has been earlier discussed [11]. From [11], the waveforms of DAB operating in EPS mode is plotted in Fig.3 and used for derivation of average model.

For Fig.3, various time intervals and various terms are defined as:

$_1$,t_2= ,t_3= B 4 ,t_5= , t_5= B

$_1$=— *[5]*

$_2$=—],[*[6]*

$_P$=— *[7]*

$$t_B=\frac{T_s[nV_{in}(1-\delta_o)+V_{out}(2d-1)]}{2(nV_{in}+V_{out})} \quad [8]$$

Here, *Vin*=Input side voltage, *Vout*=output side voltage, n =Turns ratio= δ_o is the phase shift between the diagonal devices on primary side or inner phase shift, d=duty ratio of DAB operation, or phase shift between primary and secondary side, L= the inductance of primary winding plus the referred inductance value of secondary winding, T_s =Semi time period, I_P=Peak value of inductor current, $I_f = I_P - I_{L1}$, I_r=$I_P - I_{L2}$

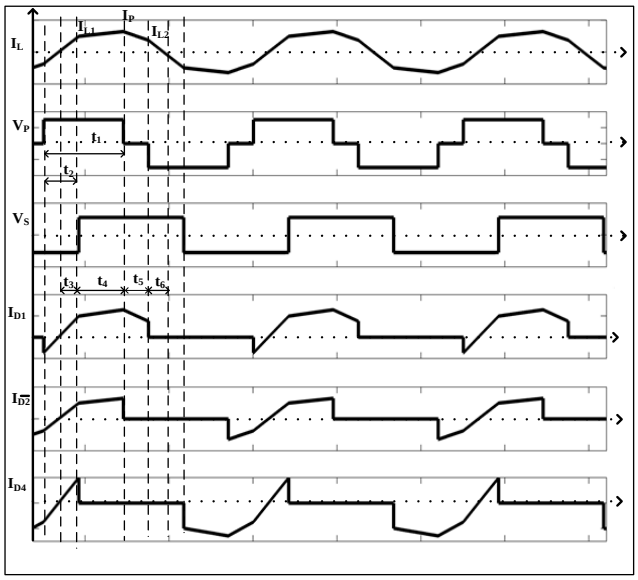

Fig.3.Operating waveforms of DAB in EPS mode, Inductor current (I_L), Primary Voltage (V_P), Secondary Voltage (V_S), Switch Current (I_{D1}), Switch Current (I_{D2}), Switch current (I_{D4})

Now the DAB operating in EPS mode can be expressed in terms of average output current (I_{oa}) and (I_{RMS})=RMS value of output current.

$$I_{oa}=\frac{nT_sV_{in}[d-d^2-d\delta_o+\frac{\delta_o}{2}-\frac{{\delta_o}^2}{2}]}{L} \quad [9]$$

$$I_{RMS}=\frac{1}{T_s}\left[\frac{(I_{L1}{}^2)(dT_s-t_B)}{3}+(T_s-\delta_oT_s-dT_s)\left(I_{L1}{}^2+\frac{I_r{}^2}{3}+I_{L1}I_r\right)+\delta_oT_s\left(I_P{}^2+\frac{I_f{}^2}{3}-I_PI_f\right)+\frac{I_{L2}{}^2t_B}{3}\right] \quad [10]$$

(d)DAB parameter design

The design of DAB consists of selection of Input capacitor and output capacitor which are discussed in this section.

$$C_{input}=(\Delta I_LT_{sw})/8\Delta V_o \quad (11)$$

C_{input}=Input side capacitor value, ΔI_L=Peak to Peak ripple in inductor current

T_{sw}=Total time period ($1/f_{sw}$), f_{sw}=switching frequency

Now taking f_{sw}=20000, ΔV_o=1% of 35V (output voltage)=0.35V, ΔI_L=<20%(15.6),we get

$C_{input}=\frac{15.6*1}{20000*8*.35}=\frac{15.6}{56000}$=278.57μF, we are taking it at 300μF for slight less ripples

$$C_{output}=(I_oDT_{sw})/\Delta V_o \quad (12)$$

C_{output}=Output side capacitor value, I_o=Output current value, D=Duty ratio corresponding to outer phase shift between the two bridges, T_{sw} =Total time period($1/f_{sw}$), f_{sw} = switching frequency, ΔV_o=Peak to Peak ripple in output voltage.

Now taking f_{sw}=20000, ΔV_o=1% of 35V (output voltage)=0.35V, ΔI_L=<20%(15.6),we get

$C_{output}=\frac{17.5*.94*1}{20000*0.18}=\frac{16.45}{3600}$=4569.44μF, C_{output} is taken as 4500μF.

In EPS mode, transmitted power is given by

$$P = NV_1V_2[D_2(1-D_2)+1/2D_1(1-D_1-2D_2)]/2f_sL \quad (13)$$

Where, V_1=Primary side voltage, V_2=Secondary side voltage, N=Transformation ratio of isolation transformer, D_1=Inner phase shift duty ratio in primary bridge, D_2=Outer phase shift duty ratio between primary bridge voltage and secondary bridge voltage, f_s=Switching frequency, L=Leakage inductance of primary plus referred value of secondary leakage inductance on primary side.

(e) Modelling of Battery:

The combination of two lead acid batteries acts as the energy storage system. Both batteries are connected in series thus forming the storage system and are placed at the low voltage bus as shown in Fig.1. Following are the governing equations of the used battery.

• Discharge:

$$V_{bo}=V_i-R*i-P\frac{q}{q-it}*(K+i*)+x(t) \quad (14)$$

$$x(t) = B*|i(t)|*(-x(t)+A\cdot*u(t)) \quad (15)$$

x(t) = Exponential zone voltage (V),i(t) = Battery current (A),u(t) = Charge or discharge mode

Charge:

$$V_{batt}=V_i-R*i-P\frac{q}{q-it}*(K)-P\frac{q}{K-.1q}(i*)+x(t) \quad (16)$$

V_{bo}= battery voltage (V),V_i = battery constant voltage (V),P = polarisation constant (V/(Ah)) or polarization resistance (Ω),q= battery capacity (Ah),K=it = actual battery charge (Ah)

A=exponential zone amplitude (V),B= exponential zone time constant inverse $(Ah)^{-1}$,R=internal resistance (Ω),i = battery current (A),i*= filtered current (A)

3. Closed loop control Techniques and selection of optimum duty ratio in operating zone

3.a)Closed loop controller design and operation

Various linear controllers based upon the target variables (input current, output power, output

current, inductor current etc) had been implemented earlier for control of dual active bridge converters. Input current is controlled to ensure equal current sharing among parallel connected DAB's [23].Output current control is effectively used to charge and discharge a battery load [24].In the present work output voltage across the load is regulated by the controller and the required phase shift between the two bridges is also provided by the controller. The closed loop controller used for regulating the load voltage is shown in Fig.4.

From the diagram it is clear that first of all the controller maintains the load voltage at the reference voltage level and the power flows from the solar panel to load and battery storage. This direction of power flow is the forward power flow direction. Thus in the forward power flow direction energy is stored in the battery. Also while maintaining the output voltage at the reference value the controller provides the necessary phase shift between the bridges.

Now, a step change in load is made and load demand is increased subsequently. Now the battery starts discharging and power flows from the battery to the load so that the load demand is met. Thus reversal in direction of power flow takes place and power flows in reverse direction. Thus in the reverse power flow direction power flows from the LV (low voltage) bus to the HV (high voltage) bus while in the forward direction, power was flowing from the HV bus to the LV bus.

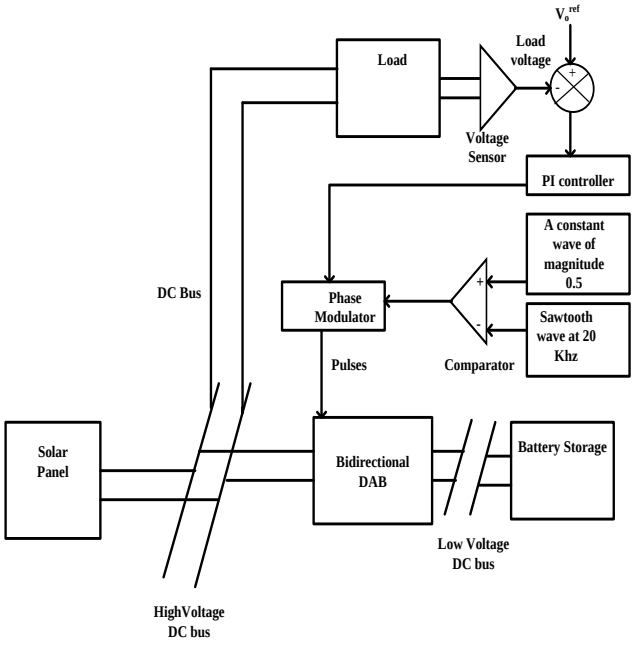

Fig.4.Schematic diagram of closed loop controller for DC-microgrid control.

Before commencing the discussion of optimum operating zone for converter operation and selection of optimum duty ratio the dependence of control parameters on various DAB components and system parameters is discussed.

From the harmonic analysis done in [25] the harmonic model for DAB is developed which is represented in (17).

$$\frac{d\Delta V_{out}(t)}{dt}=A\Delta V_{out}+B_{\emptyset}\Delta\emptyset+G\Delta i_{load} \quad (17)$$

$$A=\frac{8}{C\pi^2}\left(\frac{Np}{N_s}\right)^2\sum_{n=0}^{N}\frac{\cos\theta_n}{Z\,[n](2n+1)^2},$$

$$B_{\emptyset}=\frac{8Vin}{C\pi^2}\frac{Np}{N_s}\sum_{n=0}^{N}\frac{\sin(\theta_n-[2n+1]\emptyset)}{Z\,[n](2n+1)^2},\ G=-\frac{1}{C}$$

Here, $V_{in}(t)$=Input side voltage, $V_{out}(t)$=output side voltage, i_L=Inductor current, R_L=Resistance of leakage inductance, L=Leakage inductance, N_p=Number of turns in the Primary Side Winding. N_s=Number of turns in the Secondary Side Winding, $\emptyset =$ phase difference between primary side voltage and secondary side voltage, Z[n]=Impedance at nth harmonic,$\theta_n = \tan^{-1}\frac{[2n+1]\omega_s L}{R_L}$, ω_s is the switching frequency of the square wave, n=integers representing the number of harmonics, C=output capacitor, $i_{load}(t)$= Load current.

Now the PI controller parameters are optimised based on this harmonic model. The controller bandwidth is kept high for enhancing the performance of PI controller. The controller bandwidth(ω_c) is the frequency at which the forward transfer function gain is unity. Also the transient response of controller is affected by the phase margin(δ_m) of the controller at the crossover frequency.

The forward path transfer function is stated as:

$$T(s)=K_P\left(1+\frac{1}{sT_r}\right)e^{-sT_d}\frac{B_{\emptyset}T_P}{1+sT_P} \quad (18)$$

K_P=Proportional gain

T_r=Integrator gain

$T_P=\frac{-1}{A}$, e^{sT_d}=Unity gain delay function.

Maximum bandwidth is calculated by equating the phase at this frequency to the desired phase margin. Upon simplifying

$$\delta_m=\tan^{-1}(\omega_c T_r)-\omega_c T_d \quad (19)$$

Now phase contribution of integrator is maximized for maximizing ω_c, thus $\tan^{-1}(\omega_c T_r)=\frac{\pi}{2}$

$$\text{So, } \omega_c=\frac{\frac{\pi}{2}-\delta_m}{T_d} \quad (20)$$

For maximizing phase contribution of integrator, integrator time constant becomes a decade below ω_c.

$$T_r=\frac{10}{\omega_c} \quad (21)$$

Now the forward transfer function gain is equated to unity at the desired phase margin and crossover frequency for obtaining the value of proportional gain constant K_P.

$|T(j\omega_c)|= 1$

$$K_P=\frac{\omega_c}{B_\emptyset}, \text{where} B_\emptyset=\frac{8Vin}{C\pi^2}\frac{Np}{N_s}\sum_{n=0}^{N}\frac{\sin(\theta_n-[2n+1]\emptyset)}{Z[n](2n+1)^2} \quad (22)$$

From the above expression it becomes clear that the number of turns in the primary as well as secondary winding, the system input voltage, and the leakage inductance of the transformer greatly affects the value of proportional gain constantK_P. Also from the expression of $B_\emptyset$ it becomes obvious that the proportional gain depends on the phase shift between the primary and the secondary side. Thus a single value of K_P is not suitable for regulating the output voltage at the reference value and operation of converter at a high efficiency is not possible in the entire operating range. Thus a trade-off has to be done between the converter efficiency and output voltage. This will become evident in the process of duty ratio selection in the entire operating zone.

Values of proportional and integral gains are given in TableI. Also the error signal input to PI controller is shown in Fig.5.The error signal shows the operation of closed loop controller.

Table I System parameters

K_P	3
K_I	12

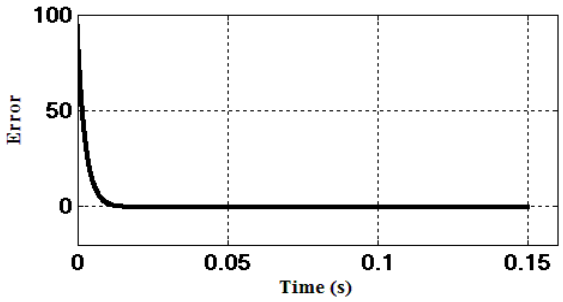

Fig.5. Error signal to PI controller

3.b) Duty ratio selection

In case of EPS control mode, duty ratio is varied in three range, first inner phase shift is kept at three values namely, D_1 =0.3,0.5&0.75.After this the outer phase shift(D_2) is varied from0.1 to0.95.This can be observed in Table II,III,IV.

Input power is the power injected by the solar PV. Storage power is the power stored in the battery storage system. Load power is the power supplied to the linear load. In the forward power flow mode some part of injected power is stored in battery and rest part of power is fed to the load. Thus power through the DAB flows from the HV bus to the LV bus. While in the reverse power flow mode battery as well as solar PV feeds the load thus power through the DAB flows from the LV bus to the HV bus.

Table II
Efficiency and duty ratio for DAB with EPS control in forward mode for D_1=0.3.

Duty Ratio	Input Power(P_{in} in VA)	Storage Power(P_s in VA)	Load Power(P_l in VA)	Efficiency(η in %)	Output Voltage(V_{out}in V)
D_2=0.1	1116.8	173	1270	88.55	112.9(Reversal)
D_2=0.25	1116.5	35	1269.5	22.87	112.6(Reversal)
D_2=0.35	1032.92	1021.5	0	0	112.9(Boundary of reversal)
D_2=0.40	1020.08	16.2	991.6	56.88	99.55
D_2=0.5	992.53	48.2	931.08	78.43	96.48
D_2=0.53	983.81	57.7	912.78	81.23	95.53
D_2=0.75	924.01	110.3	796.05	86.2	89.24
D_2=0.85	920.85	110.5	790.26	84.6	92.83
D_2=0.90	927	104	801.56	82.91	89.56

Table III
Efficiency and duty ratio for DAB with EPS control in forward mode for D_1=0.5

Duty Ratio	Input Power(P_{in} in VA)	Storage Power(P_s in VA)	Load Power(P_l in VA)	Efficiency(η in %)	Output Voltage(V_{out}in V)
D_2=0.1	1131	212	1343	81.5	115.8(Reversal)
D_2=0.25	1130	215	1345	84.05	115.5(Reversal)
D_2=0.35	986.24	58.2	917.85	85.09	95.82
D_2=0.40	962.42	81.5	869.4	87.61	93.23
D_2=0.53	899.6	133.2	752.03	90.26	86.73
D_2=0.75	860.42	155	685	88.36	82.75
D_2=0.85	876.95	140.5	712.76	85.57	84.42
D_2=0.95	914.32	109.5	770.35	76.06	88.24

Table IV
Efficiency and duty ratio for DAB with EPS control in forward mode for D_1=0.75

Duty Ratio	Input Power(P_{in} in VA)	Storage Power(P_s in VA)	Load Power(P_l in VA)	Efficiency(η in %)	Output Voltage(V_{out}in V)
D_2=0.1	1139.65	302	1407	88.52	118.6(Reversal)
D_2=0.20	982.72	63.8	910.52	88.36	95.42
D_2=0.30	914.14	125.2	778.02	91.98	88.20
D_2=0.40	859.25	162.2	683	92.02	82.64
D_2=0.50	824.04	180.4	626.25	91.20	79.14
D_2=0.53	817.6	183.4	616.2	91.06	78.5
D_2=0.75	831.65	167.9	638.25	86.81	79.90
D_2=0.85	872.88	138	706	82.78	84.06
D_2=0.95	933.75	87.5	814.18	73.17	90.22

From the table it can be observed that at some

duty ratios (D_2=0.1,0.25) there is reversal happening. Reversal means power flow direction reverses, that implicates power flow from storage to source in case of forward power flow. The duty ratios D_1=0.75,D_2=0.20 is selected as the operating duty ratio as the efficiency is highest at this value. In EPS control mode for reverse power flow again three duty ratios are selected namely, D_1 =0.3, 0.5&0.75. After this the outer phase shift (D_2) is varied from0.15 to 0.95.This can be observed in Table V, VI, VII.

Table V
Efficiency and duty ratio for DAB with EPS control in forward mode for D_1=0.3.

Duty Ratio	Input Power(P_{in} in VA)	Storage Power(P_s in VA)	Load Power(P_l in VA)	Efficiency(η in %)	Output Voltage(V_{out}in V)
D_2=0.15	887.3	45.73	839.76	96.19	85.47
D_2=0.25	915.5	17.18	897.2	93.88	88.34(unstable)
D_2=0.35	942.48	13.54	954.76	90.66	91.14
D_2=0.45	968.20	44.34	1012.53	96.39	93.85
D_2=0.5	980.43	63	1041.07	96.25	95.17
D_2=0.75	978.83	87	1037.4	67.31	94.89(unstable)
D_2=0.85	978.8	86	1037.3	68.02	94.89(unstable)
D_2=0.95	978.75	85	1037.4	69	94.98

Table VI
Efficiency and duty ratio for DAB with EPS control in forward mode for D_1=0.5.

Duty Ratio	Input Power(P_{in} in VA)	Storage Power(P_s in VA)	Load Power(P_l in VA)	Efficiency(η in %)	Output Voltage(V_{out}in V)
D_2=0.15	904.3	27.6	874	89.31	87.19(Not sufficient)
D_2=0.25	947.7	21	966.29	88.52	91.68
D_2=0.35	988.02	74.2	1059.24	95.98	95.99
D_2=0.45	978.84	96	1037.4	61	95.14
D_2=0.5	978.82	98	1037.34	59.71	94.94(Unstable)
D_2=0.75	978.7	98	1037.35	59.84	94.98(Unstable)
D_2=0.85	978.83	97	1037.3	60.27	95.1(Unstable)
D_2=0.95	978.8	93	1037.3	62.90	95.01(Unstable)

Table VII
Efficiency and duty ratio for DAB with EPS control in forward mode for D_1=0.75.

Duty Ratio	Input Power(P_{in} in VA)	Storage Power(P_s in VA)	Load Power(P_l in VA)	Efficiency(η in %)	Output Voltage(V_{out}in V)
D_2=0.15	963.83	43.4	1002.5	89.10	93.4
D_2=0.18	981.2	66.6	1043	92.8	95.25
D_2=0.30	978.82	100	1037.32	58.8	95.18
D_2=0.45	898.72	30	862.7	83.28	86.63(Not sufficient)
D_2=0.6	978.8	110	1037.2	53.90	94.99(Unstable)
D_2=0.75	978.82	110	1037.2	53.90	94.99(Unstable)
D_2=0.95	978.82	105	1037.2	55.60	94.99(Unstable)

From the table it is evident that the EPS control mode for reverse power flow has a large number of unstable points at various duty ratios (D_2=0.60, 0.75, 0.95 for D_1=0.75, D_2=0.5, 0.75, 0.85, 0.95 for D_1=0.5& D_2=0.25,0.75,0.85 for D_1=0.3).Also sufficient power is not transferred from LV side to HV side at duty ratio of D_2=0.45 for D_1=0.75and D_2=0.15 for D_1=0.50.As the efficiency is highest at D_1=0.3, D_2=0.5,hence this is taken as the operating duty ratio.

4.Performance Evaluation

4.a) EPS Technique

The dual active bridge converter in EPS mode is simulated with solar PV array at input side or High Voltage (HV) side and battery at Low voltage (LV) side using MATLAB/SIMULINK and SimPowerSystems software. Load is connected at the high voltage bus. The system parameters are specified in Table VIII.

Table VIII System parameters

	EPS(forward)	EPS(reverse)
V_{in}(Input voltage)	95.42(HV side)	65.92V(LV side)
V_{out}(Output voltage)	66.92V(LV side)	95.17V(HV side)
C_{in}(Input capacitor)	300µF	4500µF
C_{out}(Output capacitor)	4500 µF	300 µF
L(Leakage inductor)	450 µH	450 µH
N(Tranformer ratio)	300:100	100:300
SOC(State of charge)	90%	90%
P_{in}(VA)	982.72	980.43
P_{load}(VA)	910.52	1041.07
Storage Power(VA)	63.8	63
Load Voltage(V)	95.42	95.17
Efficiency (%)	88.36	96.25

The DAB waveforms are shown in Fig.6 and Fig.7 for forward as well as reverse power flow mode respectively

4.a.1.Forward conduction mode: In the forward mode, Solar PV-array on the high voltage (HV) side is at the voltage of 95.42V and the battery on the low voltage (LV) side is maintained at a voltage of 66.92V. The transformation ratio in this mode is 300:100.

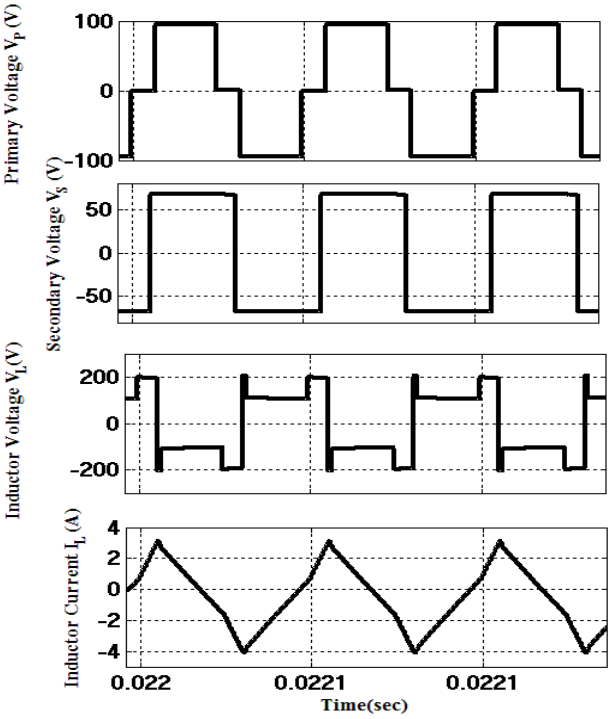

Fig.6. Waveforms of Primary voltage, Secondary voltage, Inductor voltage, Inductor current for forward power flow.

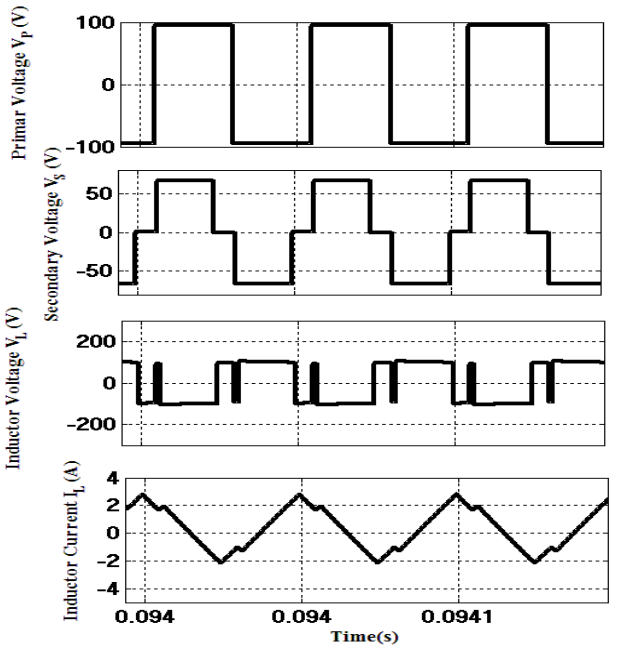

Fig.7.Waveforms of Primary voltage, Secondary voltage, Inductor voltage, Inductor current for reverse power flow.

During this mode of operation, the solar PV array injects a power of 982.72VA. This is shown in Fig.8.

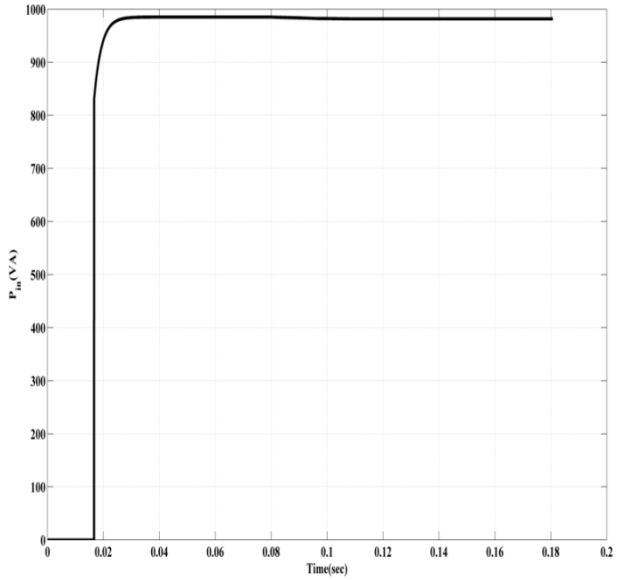

Fig.8. Input power of Solar PV array

The load consumes a power of 910.52VA. 63.8VA is stored in battery storage system. Battery characteristics is shown in Fig.9.It can be shown from Fig.9 that during forward mode, the SOC of the battery on the LV side increases, the battery current is charging(current having negative value), which depicts power flow from the high voltage (HV) side to the low voltage(LV) side.

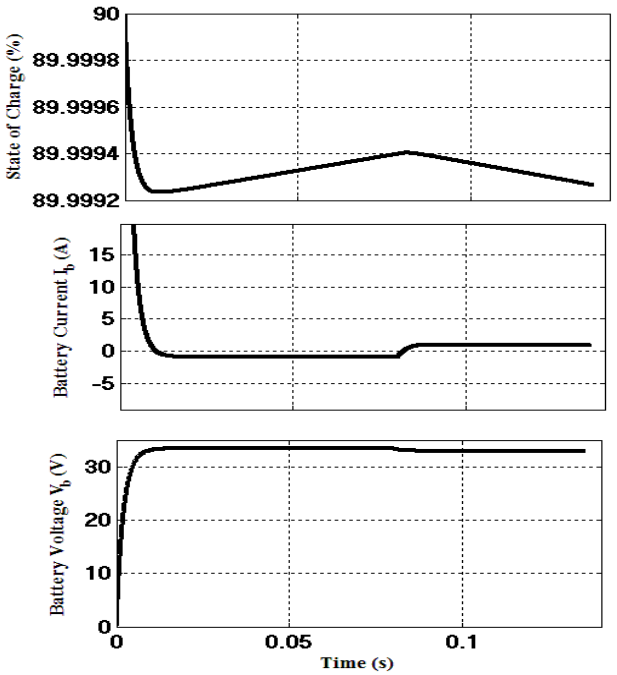

Fig.9. Battery characteristics showing State of charge of battery, Battery current, Battery voltage on the LV side

4. a.2.Reverse conduction mode: In the reverse power flow mode, at optimum duty ratio battery on LV side is at a voltage of 65.92 V and delivers a power of 63VA and this is the input in reverse mode, and the Solar PV on HV side supplies a power of

980.43VA.The transformation ratio in this mode is 100:300.The power consumed by load after step variation in load becomes 1041.07VA. Thus a power of 60.64VA is delivered by the converter. Thus the efficiency of converter in reverse mode is (60.64/63=96.25%).During this mode of operation, the SOC of battery on the LV side decreases, thus indicating the power transfer from the low voltage (LV) side to high voltage (HV) side. The battery current on the LV side is discharging (current having positive value). Also from the power characteristics in Fig.10, it is clear that the battery on the low voltage (LV) side is absorbing power in the forward power flow mode and is delivering power in the reverse power flow mode.

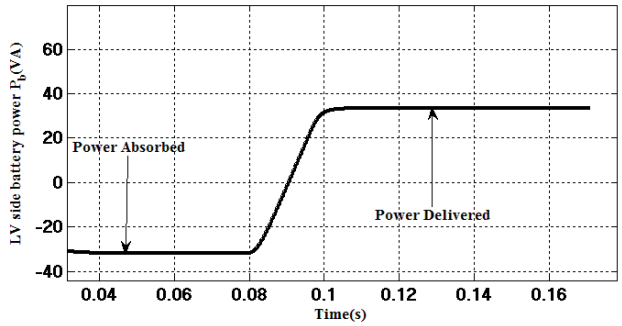

Fig.10. Power characteristics of battery on the LV (low voltage side)

Thus it becomes clear that bidirectional power flow is taking place in DAB having solar PV array at one end and lead acid battery on the other the side in EPS control mode.

Also the performance of closed loop controller in order to maintain load voltage at 95 volts can be seen in Fig.11.

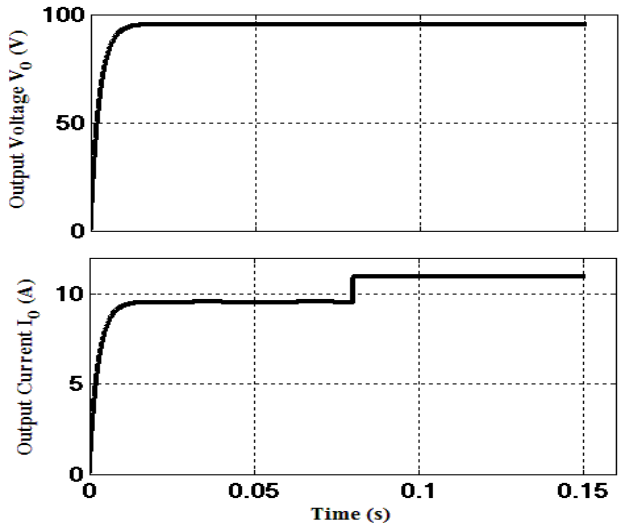

Fig.11. Load voltage (V) and load current (A) vs time (s) for EPS contol mode in DC microgrid.

From the above figure it becomes clear that the voltage at load terminals remains constant despite the load current has increased.

5.RT-LAB Experimental Results and Discussions

The proposed controller is applied to DAB and MATLAB/Simulink results are validated with a real time digital simulator. The laboratory set-up of real time simulator OPAL-RT along with host PC and four channel digital storage oscilloscope is shown in Fig.12. OPAL-RT consists of X11SSM-E-F-O Supermicro Server Motherboard, Intel Xeon 3.5 GHz processor and Intel Socket H4 LGA-1155 µTAX working under RT-Lab environment. The output waveforms of OPAL-RT simulated models are obtained on a 4 channel digital storage oscilloscope (DSO). OPAL-RT creates real time conditions by solving the mathematical equations in smaller time intervals.

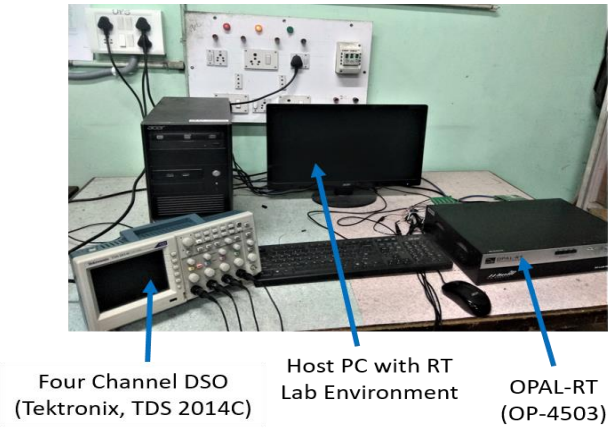

Fig.12. Laboratory set-up of OPAL-RT with host PC and DSO.

Simulation waveforms for DAB (primary voltage, secondary voltage, inductor voltage, inductor current) and battery(state of charge, battery current and battery voltage) are well supported by real time simulation results obtained from OPAL-RT. DAB converter waveforms in EPS mode are shown in Fig.13 (a),(b) for forward direction of power flow. The phase shift between the primary side voltage and secondary side voltage is evident in real time simulation results. Similarly the converter waveforms for EPS mode in the reverse power flow direction are shown in Fig.13 (c),(d).

Similarly battery voltage, battery current for battery at the LV side is shown in Fig.14 (a). Battery power for the battery is shown in Fig.14 (a) depicting the bidirectional power flow among the battery and the source. Input power along with battery power is shown in Fig.14 (b).

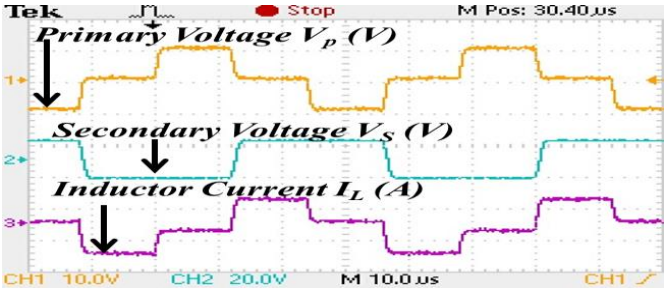

a

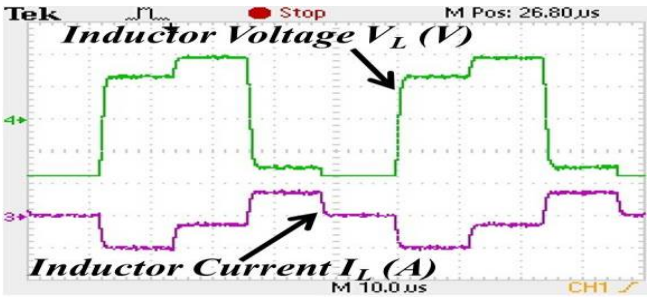

b

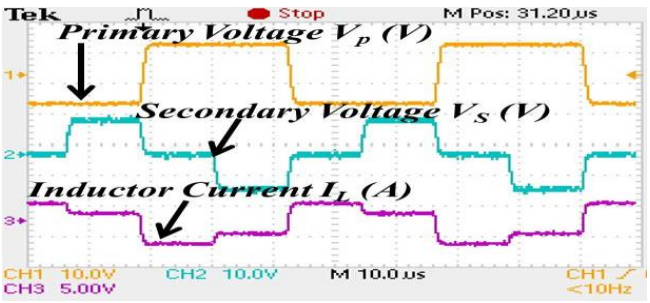

c

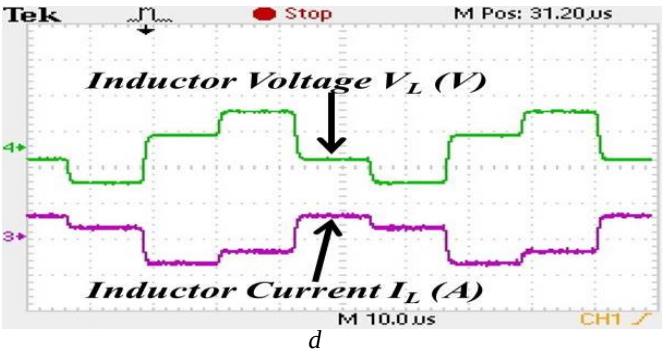

d

Fig.13.(a) Waveforms in forward direction showing Primary Voltage, Secondary Voltage and Inductor Current
(b) Waveforms in forward direction showing Inductor Voltage and Inductor Current
(c) Waveforms in reverse direction showing Primary Voltage, Secondary Voltage and Inductor Current
(d)Waveforms in reverse direction showing Inductor Voltage and Inductor Current

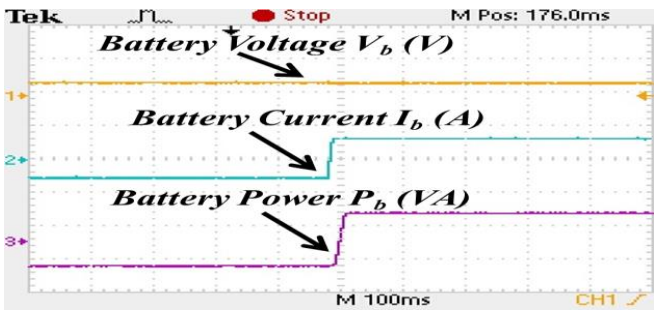

a

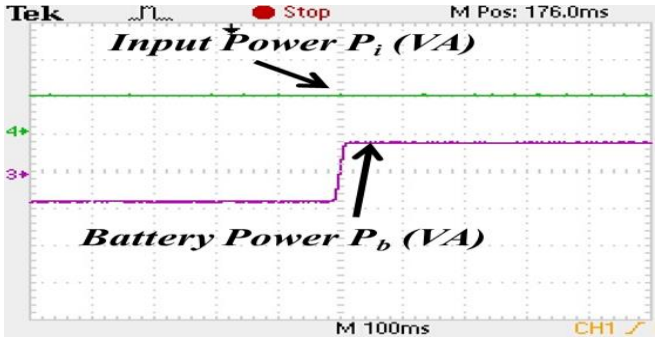

b

Fig.14. (a) Battery voltage, battery current, battery power for LV side battery
Fig.14. (b) Input power and battery power

Output Voltage along-with output current is shown in Fig.15.

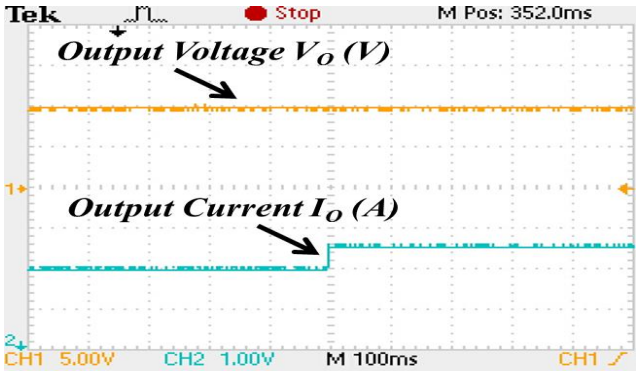

Fig.15.Output Voltage and Output Current

Conclusions

From the analysis of DAB with EPS control techniques, it can be concluded that DAB with EPS control technique is suitable for application as a power electronics interface in a DC microgrid. It can be seen from the above work that bidirectional power transfer in a DC microgrid is feasible for DAB in EPS mode. The efficiency for DAB in EPS control mode is 88.36% and it is 96.25% in the reverse mode.

In the forward direction solar PV supplies the load demand as well as excess energy is stored in the battery. When a step increase in load occurs, the battery discharges and supplies the increased load demand in the reverse power flow direction.

Also the optimum duty ratio for the bidirectional operation of DAB has been obtained by the closed loop controller in the operating range by selecting the output voltage as the target variable.

In the present work, the SOC of the battery, battery voltage and battery current are shown. The changes in SOC (increasing while charging and decreasing while discharging) and the changes in battery current (negative for charging and positive for discharging) make the bidirectional power flow evident.

The above mentioned simulation model along with simulation results are verified with real time simulation results obtained on a 4 channel DSO from the OPAL-RT.

Thus bidirectional power flow in a DC-microgrid is achieved using a DAB working in EPS mode.

References

[1] Hofer.J., Svetozarevic.B. and Schlueter.A., *Hybrid AC/DC building microgrid for solar PV and battery storage integration*, In: 2017 IEEE Second International Conference on DC Microgrids (ICDCM), Nuremburg, 2017, pp. 188-191.

[2]Kondrath.N., *Bidirectional DC-DC converter topologies and control strategie for interfacing energy storage systems in microgrids: An overview*, In: *2017 IEEE International Conference on Smart Energy Grid Engineering (SEGE)*,Oshawa, ON, 2017 pp. 341-345.

[3] Fusheng. Z and Naayagi.T.R., *Power Converters for DC Microgrids – Modelling and Simulation*, In:2018 IEEE Innovative Smart Grid Technologies - Asia (ISGT Asia), Singapore, 2018, pp. 994-999.

[4]Leal..C.W.,*A control system for battery current sharing in DC microgrids with DC bus voltage restoration*, In: 2017 Brazilian Power Electronics Conference (COBEP), Juiz de Fora, 2017, pp. 1-6.

[5] Korompili.A. and Monti.A., *Analysis of the dynamics of dc voltage droop controller of dc-dc converters in multi-terminal dc grids*, In:2017 IEEE Second International Conference on DC Microgrids (ICDCM), Nuremburg, 2017, pp. 507-514.

[6]Doncker.D.A.A.W.R.,Divan.M.D,and Kheraluwala.H .M., *A three phase soft-switched high-power-density dc/dc converter for high power applications*, In:IEEE Transactions on Industrial. Appl., vol. 27, no. 1, pp. 63–73,Jan./Feb. 1991.

[7] Shi.H *et al.*, *Minimum-Backflow-Power Scheme of DAB-Based Solid-State Transformer With Extended-Phase-Shift Control*, In: IEEE Transactions on Industrial Applications, vol. 54, no. 4, pp. 3483-3496, July-Aug. 2018.

[8] Nalamati.S.C and Gupta.R., *Isolated bidirectional battery converter control for standalone solar PV applications*, In:2018 IEEMA Engineer Infinite Conference (eTechNxT), New Delhi, 2018, pp. 1-5.

[9] Alonso.R.A., Sebastian.J, Lamar.G.D., Hernando.M.M. and Vazquez.A., *An overall study of a Dual Active Bridge for bidirectional DC/DC conversion*, In:2010 IEEE Energy Conversion Congress and Exposition, Atlanta, GA, 2010,pp.1129-1135.

[10]Mi.C.,Bai.H.,Wang.C.,andGargies.S., *Operation, design and control of dual H-bridge-based isolated bidirectional dc-dc converter* , In: IET Power Electron., vol.1, no.4, pp.507–517,Apr. 2008.

[11]Naayagi.T.R., Forsyth.J.A. and R. Shuttleworth.R., *Performance analysis of extended phase-shift control of DAB DC-DC converter for aerospace energy storage system*, In:2015 IEEE 11th International Conference on Power Electronics and Drive Systems, Sydney, NSW, 2015, pp. 514-517.

[12] ZhaoB., YuQ. and SunW., *Extended-Phase-Shift Control of Isolated Bidirectional DC–DC Converter for Power Distribution in Microgrid*, In: IEEE Transactions on Power Electronics, vol. 27, no. 11, pp. 4667-4680, Nov. 2012.

[13] Askarian.I., Helmuth.T., Palevani.M., Knight.A. and Kaviri.M.S., *Hybrid modulation technique for Dual-Active-Bridge DC-DC converters to achieve full ZVS over wide range of operating conditions*, In:2017 IEEE 8th International Symposium on Power Electronics for Distributed Generation Systems (PEDG), Florianopolis, 2017, pp. 1-5.

[14] Iyer.M.V., Gulur.S. and Bhattacharya.S., *Hybrid control strategy to extend the ZVS range of a dual active bridge converter*, In:2017 IEEE Applied Power Electronics Conference and Exposition (APEC), Tampa, FL, 2017, pp. 2035-2042.

[15] Hirose.T. and Matsuo.H., *A consideration of bidirectional superposed dual active bridge dc-dc converter*, In: The 2nd International Symposium on Power Electronics for Distributed Generation Systems, Hefei, 2010, pp.39-46.

[16]Zhao.B., Song.Q.,and Liu.W., *Power characterization of isolated bidirectional*

dual-active-bridge dc-dc converter with dual-phase-shift control, In: IEEE Trans. Power Electron., vol. 27, no. 9, pp. 4172–4176, Sep.2012.

[17] Krismer.F. and Kolar.W.J., *Accurate small-signal model for the digital control of an automotive bidirectional dual active bridge,* In: IEEE Trans. Power Electron., vol. 24, no. 12, pp.2756–2768, Dec.2009.

[18]Hebala.M.O.,Aboushady.A.A.,Ahmed.H. K.,Burgess.S. and Prabhu.R., *Generalized Small-Signal Modelling of Dual Active Bridge DC/DC Converter,* In:2018 7th International Conference on Renewable Energy Research and Applications (ICRERA), Paris, 2018, pp.914-919.

[19] Cooper.S., Klem.A., Nehrir.H.M. and Ga.H., *An improved state-space averaged model of a dual active bridge converter for use in acausal system modeling,* In:2016 North American Power Symposium (NAPS), Denver, CO, 2016, pp. 1-5.

[20] Tian.Qi., Huang.Q.A. and Bai.H., *Time-varying full-order state-space modeling of variable-switching-frequency control for single-phase single-stage dual-active-bridge based AC/DC converter,* In:IECON 2016 - 42nd Annual Conference of the IEEE Industrial Electronics Society, Florence, 2016, pp. 1435-1440.

[21]Skouros.I., Bampoulas.A. and Karlis.A., *A bidirectional dual active bridge converter for V2G applications based on DC microgrid,* In:2018 Thirteenth International Conference on Ecological Vehicles and Renewable Energies (EVER), Monte-Carlo, 2018, pp. 1-9.

[22] Saxena.N., Singh.B. and Vyas.L.A., *Integration of solar photovoltaic with battery to single-phase grid,* In: IET Generation, Transmission & Distribution, vol. 11, no. 8, pp. 2003-2012, 1 6 2017.

[23] Z. H., D.T., S.T.S., and Khambadkone.A., *Interleaved bi-directional dual active bridge dc-dc converter for interfacing ultra-capacitor in micro-grid application,* In: Proc. 2010 IEEE International Symposium on Industrial Electronics (ISIE), 2010, pp. 2229-2234.

[24] Kunrong.W., Lizhi.Z., Dayu.Q., Odendaal.H., Lai.J., and Lee.C.F.,*Design, implementation, and experimental results of bi-directional full-bridge dc/dc converter with unified soft-switching scheme and soft-starting capability,* In:Proc. 31st IEEE Power Electronics Specialists Conference (PESC), vol. 2, 2000, pp. 1058--1063.

[25] Kumar, A., Bhat, A. ,Agarwal, P., *Reduced Rule Based Fuzzy Logic Controlled Isolated Bidirectional Converter Operating in Extended Phase Shift Control for Bidirectional Energy Transfer,* In: World Academy of Science, Engineering and Technology, International Science Index 146, International Journal of Electrical, Computer, Energetic, Electronic and Communication Engineering, 13(2), pp.94 – 109,2019.